Chapter 4

DNA barcoding of Arctic bryophytes – an example from the moss genus *Dicranum* (Dicranaceae, Bryophyta)

A. S. Lang, H. (J. D.) Kruijer & M. Stech

Published in Polar Biology, 2014, 37 (8): 1157-1169

ABSTRACT

The identification of bryophytes from the Arctic is often difficult due to deviating morphologies under the extreme environmental conditions. This is especially true for species-rich and taxonomically complex genera, such as the moss genus *Dicranum*. DNA barcoding is expected to improve the identification of Arctic bryophyte species, but the optimal combination of barcoding markers for mosses in general, especially for delimiting closely related species, is still under discussion. In this paper, we test the discrimination capacity of six potential barcode markers (*rps4-trnT*$_{UGU}$, *trnL*$_{UAA}$-*trnF*$_{GAA}$, *trnH*$_{GUG}$-*psbA*, *rps19-rpl2*, *rpoB,* nrITS1-5.8S-ITS2) based on phylogenetic reconstructions of 30 *Dicranum* samples from Spitsbergen (Svalbard, Norway) and reference samples from all ten *Dicranum* species confirmed for the Svalbard archipelago and six additional Arctic *Dicranum* species. All 16 species (possibly except *D. fuscescens*), were distinguishable with bootstrap support >70% based on the combined sequence data, but none of the individual markers could delimit all included species. All Svalbard collections could be readily assigned to five species, *D. acutifolium*, *D. elongatum*, *D. laevidens*, *D. majus*, and *D. spadiceum*, respectively. It is concluded that DNA barcoding improves species identification of Arctic *Dicranum* plants, but that a combination of several markers is necessary in order to obtain reliable identification results, with the single loci ITS1, *trnL-F* and *rps4-trnT* being the most promising regions.

INTRODUCTION

Bryophytes comprise three different phylogenetic lineages of land plants, namely liverworts, hornworts, and mosses (e.g. Qiu *et al*. 2006). Of these, liverworts and mosses play an essential role in Arctic terrestrial ecosystems and constitute a major component of different types of tundra vegetation (e.g., Callaghan *et al*. 2004; Lang *et al*. 2012; Longton 1997). The Arctic bryoflora comprises a considerable diversity of approximately 700 species (Longton 1988; Frisvoll & Elvebakk 1996; Afonina & Czernyadjeva 1995; Konstantinova & Potemkin 1997).

Bryophytes, especially mosses, have been widely employed in studies of ecosystem processes and organismal interactions in (sub-)Arctic environments (e.g., Alsos *et al*. 1998; Gordon *et al*. 2001; Gornall *et al*. 2007; Jasmin *et al*. 2008; Krab *et al*. 2008; van der Wal & Brooker 2004). The Arctic has been divided into bioclimatic regions, where the High Arctic is characterized by an open herbaceous vegetation with some dwarf-shrubs on mineral soils, while the Low Arctic generally consists of a closer herbaceous vegetation, composed of dwarf and low shrubs on peat-rich soils (Walker *et al*. 2005). Biodiversity-based investigations of Arctic ecosystem processes, however, are still severely hampered by insufficient knowledge of bryophyte taxonomy and by the ability of species recognition based on morphological characters. In response to the extreme environmental conditions bryophytes display unusual growth forms and deviant gametophytic characters in the (High) Arctic. This plasticity makes morphological identification to species level difficult or even impossible (e.g., Buryová & Shaw 2005; Frisvoll & Elvebakk 1996; Hesse *et al*. 2012). This is especially true for species-rich and taxonomically complex genera such as *Bryum* Hedw., *Dicranum* Hedw. and *Schistidium* Brid. (e.g., Steere 1978; Hesse *et al*. 2012). Consequently, ecological studies have largely been limited to a few easily distinguishable species or genus-level identifications (e.g., Okitsu *et al*. 1998), or treated bryophytes as a single category without distinction of species (e.g., van der Wal *et al*. 2001). Sometimes bryophytes are even grouped with lichens and fungi as the outdated group of 'cryptogams' (e.g., Hudson & Henry 2010; Wahren *et al*. 2005; Epstein *et al*. 2004). The development of new identification tools to treat bryophytes in a more comprehensive way would surely increase the significance of ecological studies in the (High) Arctic, especially with respect to the potential of bryophytes for investigating the impact of global climate change (Tuba *et al*. 2011).

DNA barcoding is a molecular tool for species identification based on species-specific sequence differences in a short, standardized DNA region. In contrast to this original idea, however, barcoding in land plants (including bryophytes) is supposed to be based on one or two core markers plus additional information from other DNA regions where necessary (e.g., Hollingsworth *et al*. 2009, 2011). In bryophytes, especially mosses, the plastid markers recently proposed for barcoding of land plants (CBOL Plant Working Group 2009; Kress *et al*. 2005) either tend to be short (*psbA-trnH* spacer; Stech & Frey 2008; Stech & Quandt 2010), have different discrimination capacity at the species level (*rbcL*; Liu *et al*. 2010; Stech & Quandt 2010), or need more study concerning primer design and amplification strategy (*trnK/matK*, e.g., Bell *et al*. 2012). Although the optimal combination of barcoding markers for bryophytes is still under discussion (e.g., Liu *et al*. 2010; 2011; Bell *et al*. 2012; Hassel *et al*. 2013; Stech *et al*. 2013), several other molecular markers have already shown to be useful for inferring species delimitations and identifying species in bryophytes (e.g., Bell *et* al. 2012; von Cräutlein *et al*. 2011; Draper & Hedenäs 2009; Stech *et al*. 2011, 2013).

Dicranum (Dicranaceae) is a large genus belonging to the second largest subclass of mosses, Dicranidae. It comprises ca. 90 species essentially found in the Holarctic (Crosby *et al*. 1999; Ireland 2007), including about 30 species in the boreo-arctic region, of which ten species were accepted for Svalbard (Frisvoll & Elvebakk 1996). Several *Dicranum* species show a high morphological variability (Hedenäs & Bisang 2004; Hedenäs *et al*. 2006; Smith 2004; Lang & Stech 2014), which renders their identification challenging, in particular in plants (Hedenäs *et al*. 2006; pers. obs.). Previous phylogenetic studies revealed low sequence divergence in commonly employed plastid markers (La Farge *et al*. 2002; Stech *et al*. 2006). The nuclear ribosomal ITS region allowed

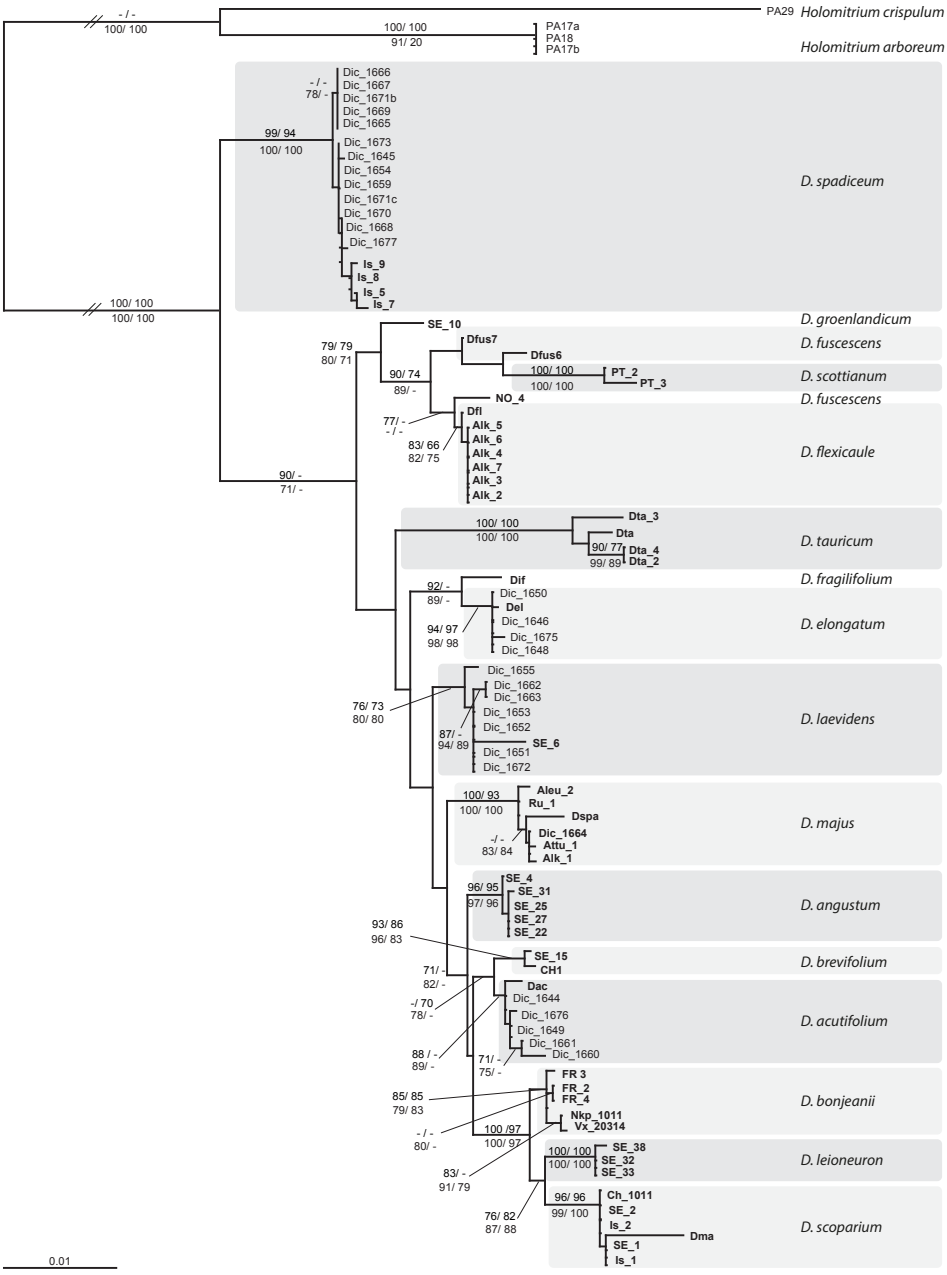

FIG. 1. Single optimal maximum likelihood phylogenetic reconstruction inferred from combined chloroplast and nrITS sequence data of *Dicranum* species, including indels coded by simple indel coding (SIC). Four specimens of *Holomitrium* were used as outgroup representatives and names in bold represent the reference samples. Numbers above branches indicate MP bootstrap support and numbers below the branch indicate ML bootstrap support, with and without indels. Branch lengths are to scale except those indicated by the symbol "//" (shortened 2 times).

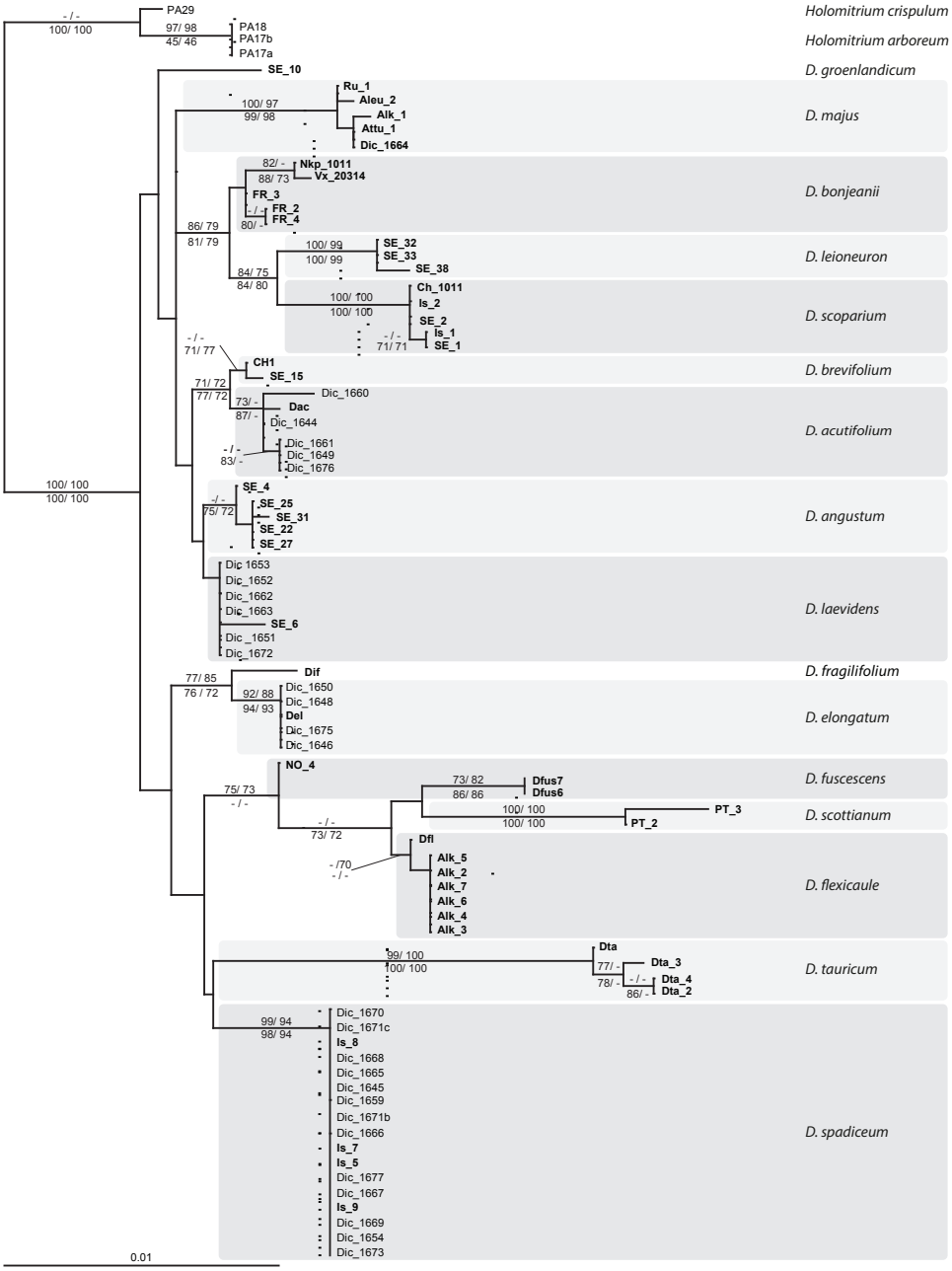

FIG. 2. Single optimal maximum likelihood phylogenetic reconstruction inferred from chloroplast sequence data of *Dicranum* species, including indels coded by simple indel coding (SIC). Four specimens of *Holomitrium* were used as outgroup representatives and names in bold represent the reference samples. Numbers above branches indicate MP bootstrap support and numbers below the branch indicate ML bootstrap support, with and without indels.

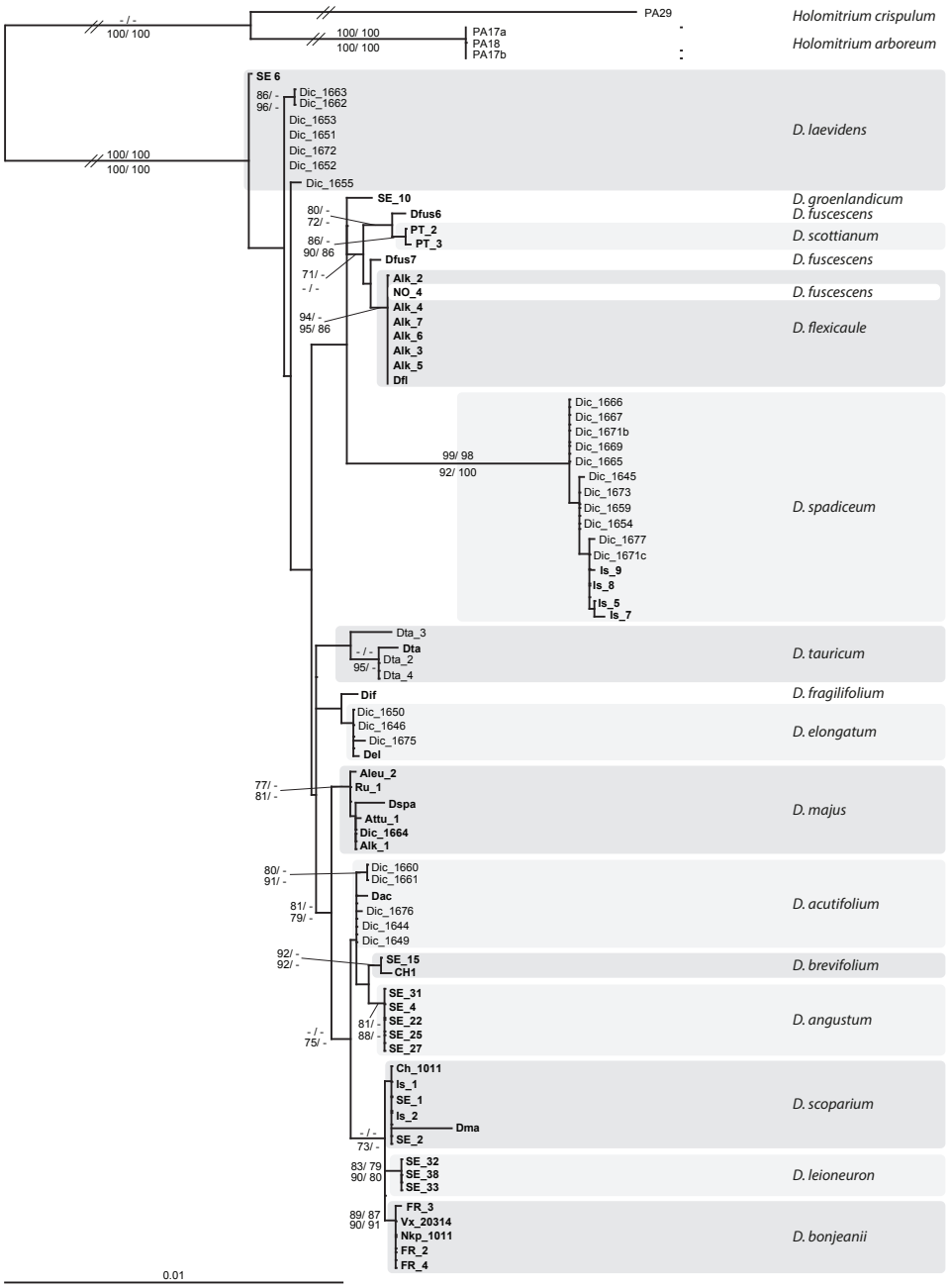

FIG. 3. Single optimal maximum likelihood phylogenetic reconstruction inferred from ITS sequence data of *Dicranum* species, including indels coded by simple indel coding (SIC). Four specimens of *Holomitrium* were used as outgroup representatives and names in bold represent the reference samples. Numbers above branches indicate MP bootstrap support and numbers below the branch indicate ML bootstrap support, with and without indels. Branch lengths are to scale except those indicated by the symbol "//" (shortened 2 times).

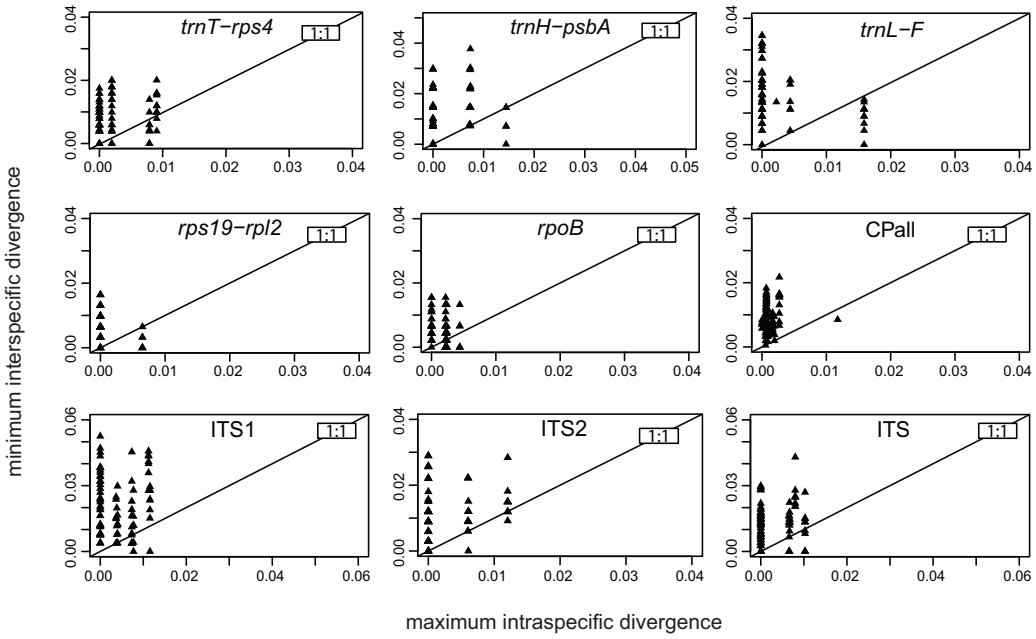

FIG. 4. Comparison of maximum intraspecific versus minimum interspecific divergence distances for *Dicranum* species pairs with more than one specimen sequenced. Genetic distances have been calculated using a K2P model of sequence evolution for *trnT-rps4*, *trnL-F*, *trnH-psbA*, *rps19-rpl2*, *rpoB*, all chloroplast markers combined (CPall), ITS and its partitions ITS1 and ITS2.

species identification in a study of Russian *Dicranum* species albeit with low support (Tubanova & Ignatova 2011; Tubanova *et al*. 2010). Most recently however, Lang & Stech (2014) showed that closely related species of the *Dicranum scoparium* Hedw. species complex were best resolved by combining five plastid regions and the nuclear ribosomal ITS region.

In the present study we aim to test how well *Dicranum* collections from the High Arctic archipelago of Svalbard can be identified to species level based on a DNA barcoding approach. Inferences are based on molecular phylogenetic reconstructions using chloroplast (*rpoB*, *trnH-psbA*, *trnL-trnF*, *rps4-trnT*, *rps19-rpl2*) and nuclear ribosomal ITS sequences from Svalbard and reference collections. The reference sequences were generated from well-identified, morphologically typical specimens from temperate to boreal regions. Furthermore, we examine the species discrimination efficacy of the six markers individually based on phylogenetic inference and comparison of maximum intraspecific versus minimum interspecific genetic distances.

MATERIALS AND METHODS

Sampling— According to the most recent checklist of the bryophytes of Svalbard (Frisvoll & Elvebakk 1996), 17 *Dicranum* species have been reported for the archipelago, of which ten were accepted in the checklist (*Dicranum acutifolium* (Lindb. & Arn.) C.Jens., *D. angustum* Lindb., *D. elongatum* Schleich. ex Schwägr., *D. flexicaule* Brid., *D. fuscescens* Sm., *D. laevidens* R.S. Williams, *D. majus* Sm., *D. scoparium* Hedw., *D. spadiceum* J.E. Zetterst., and *D. tauricum* Sapjegin), and seven were excluded due to erroneous identification (*D. bonjeanii* De Not., *D. brevifolium* (Lindb.) Lindb.,

D. fragilifolium Lindb., *D. groenlandicum* Brid., *D. leioneuron* Kindb., *D. muehlenbeckii* Bruch & Schimp., and *D. scottianum* Turner ex Scott). DNA sequences of 52 reference specimens comprising 16 out of the 17 species were compiled from earlier studies (Lang & Naciri 2010; Stech 1999; Lang & Stech 2014) or newly generated for this study (Appendix 1): *Dicranum acutifolium* (1 sample), *D. angustum* (5), *D.brevifolium* (2), *D. bonjeanii* (5), *D. elongatum* (1), *D. flexicaule* (7), *D. fragilifolium* (1), *D. fuscescens* (3), *D. groenlandicum* (1), *D. laevidens* (1), *D. leioneuron* (3), *D. majus* (6), *D. scoparium* (6), *D. spadiceum* (4), *D. scottianum* (2) and *D. tauricum* (4). The reference specimens originated from temperate to boreal regions, generally displayed morphologies typical for the respective species, and were mostly identified, or their identifications checked, by the authors or L. Hedenäs (Stockholm). *Dicranum muehlenbeckii,* however, could not be included in the analysis because of unsuccessful DNA amplification. Thirty *Dicranum* specimens from Svalbard (including one specimen already included in Lang & Stech, 2014) collected by the second and third author in Adventdalen (Longyearbyen area), Colesbukta, and Kongsfjorden (Ny-Ålesund area) in 2008-2010 were analysed (DNA numbers Dic_1644-Dic_1646, Dic_1648-Dic_1655, Dic_1659-Dic_1673, Dic_1675-Dic_1677). The collection strategy was to collect as many morphotypes as possible from the sampled areas. Four samples of *Holomitrium* Brid., one of *H. crispulum* Mart. and three of *H. arboreum* Mitt., were chosen as outgroup representatives according to earlier molecular phylogenetic reconstructions (La Farge *et al.* 2002; Stech *et al.* 2006). Voucher information and GenBank accession numbers of the DNA sequences generated from the 30 specimens are listed in Appendix 1. The nomenclature of *Dicranum* used in this study follows Hedenäs & Bisang (2004), which corresponds to the accepted species in Tropicos (Tropicos.org) and The Plant List (2013), except three species considered as synonyms in the latter two databases (*D. angustum* and *D. laevidens* as synonyms of *D. spadiceum* and *D. flexicaule* as synonym of *D. fuscescens*).

Molecular marker selection— For this study, we sequenced five chloroplast regions, i.e., partial *rpoB* gene, *trnH*$_{GUG}$*-psbA* and *rps19-rpl2* intergenic spacers, and two parts of the *trnS-F* region, namely *rps4-trnT*$_{UGU}$ spacer and *trnL-F* (*trnL*$_{UAA}$ intron and *trnL*$_{UAA}$*-trnF*$_{GAA}$ spacer), and the nuclear ribosomal nrITS1-5.8S-ITS2 region. Amplification and sequencing success as well as haplotype diversity of the chloroplast markers were inferred for *54 Dicranum scoparium* specimens by Lang & Naciri (2010). Subsequently these markers provided, together with nrITS sequences, valuable results in delimiting species of the *Dicranum scoparium* complex, based on a sampling of 111 *Dicranum* specimens (Lang & Stech 2014).

DNA extraction, amplification and sequencing— DNA was extracted from the dried leaves of a single plant using the NucleoSpin® Extract II Kit (Macherey-Nagel, Düren, Germany). Polymerase chain reaction (PCR) was performed following Lang & Stech (2014). PCR products were purified and sequenced at Macrogen Inc. (www.macrogen.com). GenBank accession numbers of all sequences are listed in Appendix 1.

Alignment and phylogenetic reconstruction— Sequences were aligned in Geneious v6.1.6 (Biomatters 2010) using 65% similarity matrix costs, and manually adjusted. Gaps were treated as missing data or coded as informative by a simple indel coding strategy (SIC) (Simmons & Ochoterena 2000) as implemented in SeqState (Müller 2004). Short hairpin-associated inversions in the *trnH-psbA* spacer were positionally separated in the alignment and not coded as indels.

TABLE 1. Alignment length (Length), number of constant characters (Constant), variable characters (Variable), parsimony-informative characters (Parsi-info) and percentage of parsimony-informative characters (% parsi-info) for nucleotide and indel matrices. Values were calculated from alignments of each marker with outgroup and ingroup only (ingr).

	trnT-rps4		*trnL-trnF*		*psbA-trnH*		*rps19-rpl2*		*rpoB*		ITS 1		ITS 2		ITS	
	ingroup		ingroup		ingroup		ingroup		ingroup		ingroup		ingroup		ingroup	
Species		15		16		16		14		16		16		16		16
Length	522	522	471	471	149	149	310	310	457	457	360	304	427	371	966	854
Constant	485	498	432	436	136	138	292	299	441	443	287	274	369	348	821	798
Variable char.	37	24	39	35	13	11	18	11	16	14	73	30	67	23	145	56
Parsi-info	33	20	35	29	9	7	11	9	12	1	49	20	42	19	96	42
% parsi- info	6	4	7	6	6	5	4	3	3	2	14	7	10	5	10	5
#indels	3	3	6	6	5	5	1	1	0	0	64	34	59	32	123	66
Parsi-info	3	3	4	5	3	3	1	1	0	0	49	28	37	20	87	53
Total parsi-info	36	23	39	34	12	10	12	10	12	10	98	48	79	39	183	95

Numbers of constant, variable and parsimony-informative sites were calculated for each locus using PAUP* v4.0b10 (Swofford 2002).

Phylogenetic analyses using Maximum Parsimony (MP) optimality criterion and maximum likelihood (ML) were performed on every marker separately (including separate analyses of ITS1 and ITS2) and the combined markers (total evidence trees *sensu* Kluge 1989), both with and without indels included. Before combining markers, we tested for incongruence by visual inspection of the separate trees and by applying an incongruence length difference test (ILD, Farris *et al.* 1994) as implemented in PAUP* with 100 replicates.

MP analyses were performed using PAUP*. Heuristic searches were performed with 100 replicates using random sequence addition, one tree held at each step and tree bisection-reconnection (TBR) branch swapping, saving up to 10,000 trees. ML analyses were carried out with RAxML v. 7.3.0 (Stamatakis *et al.* 2006) employing the raxmlGUI v.0.93 interface (Silvestro & Michalak 2012). The default GTR+Γ model was chosen for all markers. Bootstrap analyses under ML were done using the thorough bootstrap heuristics algorithm with 1,000 replicates.

Pairwise nucleotide distances between all sequences were calculated in PAUP* under the Kimura 2-parameter (K2P) model for the combined chloroplast dataset, ITS and all partitions. Maximum intraspecific distances were plotted against minimum interspecific distances for all possible species pairs with more than one specimen sequenced to infer the presence of a barcoding gap (cf. Stech *et al.* 2013).

RESULTS

Lengths of the sequenced chloroplast markers within *Dicranum* and *Holomitrium* ranged from 509-521 nucleotides for *rps4-trnT*, 449-471 nt for *trnL-F*, 136-140 nt for *trnH-*

psbA, 309-310 nt for *rps19-rpl2* and 457 nt for *rpoB*. The total plastid alignment comprised 1909 positions, of which 123 were variable, and 100 of the variable positions were parsimony-informative. Simple indel coding yielded a total of 15 additional characters, of which 11 were parsimony-informative. Hence, a total of 111 parsimony-informative characters resulted from the plastid markers. Sequences length of nrITS1-5.8S-ITS2 ranged from 747-900 nt (747-839 within *Dicranum*). The alignment comprised 1086 positions, of which 120 were removed from further calculations due to ambiguous alignment. Of the 966 remaining positions, 145 were variable and 96 of the variable positions were parsimony-informative. Simple indel coding yielded 123 characters of which 87 were parsimony informative. In total, 183 parsimony-informative characters resulted from nrITS. Respective numbers of parsimony-informative characters per plastid marker and for ITS1 and ITS2 separately are summarized in Table 1. The partitions with the most parsimony-informative characters were ITS1 (13.61%) and ITS2 (9.84%), followed by the chloroplast markers *trnL-F* (7.43%), *rps4-trnT* (6.32%), *trnH-psbA* (6.04%), *rps*19-*rpl*2 (3.55%), and partial *rpoB* gene (2.63%).

Maximum parsimony analyses with or without indels included resulted in most parsimonious phylogenetic reconstructions with similar consistency indices (combined chloroplast: CI 0.7306 versus 0.7159, ITS: CI 0.7939 versus 0.8394), indicating only a slightly higher amount of homoplasy in the indel characters in ITS. Both visual inspections of plastid versus ITS tree topologies and the ILD test ($p = 0.29$) indicated that the two datasets were congruent and could be combined.

The single optimal ML tree of the combined analysis of all markers including indels is shown in Fig. 1 (lnL = -7188.5806). The optimal ML trees calculated from the combined chloroplast markers versus ITS (lnL = -3728.5203 and lnL= -3159.2803, respectively) are shown in Figs. 2 and 3, with bootstrap support values (BS) from maximum parsimony and maximum likelihood analyses. Separate clades of all 16 included *Dicranum* species were resolved in the combined tree (Fig. 1) and the plastid marker tree (Fig. 2) according to the positions of the reference specimens, except *Dicranum fuscescens* that was resolved as paraphyletic. The ITS tree (Fig. 3) was less resolved and most clades were weakly supported. The *D. leioneuron, D. majus, D. scottianum and D. spadiceum* clades received bootstrap support of ≥70% in all three phylogenetic inferences. The *D. acutifolium, D. elongatum*, *D. scoparium*, and *D. tauricum* clades yielded high support in the chloroplast and combined analyses, whereas the *D. angustum, D. bonjeanii and D. brevifolium* clades were supported (≥80% BS) in ITS and the combined tree. The *D. flexicaule* and *D. laevidens* clades received high boostrap support (≥78%) only in the combined analysis (Table 2). High support in the combined trees was furthermore obtained for the sister group relationships of *D. elongatum* + *D. fragilifolium*, *D. flexicaule* + *D. fuscescens* + *D. scottianum*, as well as *D. bonjeanii* + *D. scoparium* + *D. leioneuron* of the *D. scoparium* complex. The Svalbard specimens clustered in five clades, namely the *D. acutifolium* (5 specimens), *D. elongatum* (4), *D. laevidens* (7), *D. majus* (1) and *D. spadiceum* (13) clades (Figs. 1-3).

Clades with more than one sequence were generally weakly supported in each of the seven single partitions (Table 2). Moreover, only six clades were recovered in at least four partitions, namely the *D. leioneuron*, *D. majus*, *D. scoparium, D. scottianum*, *D. spadiceum* and *D. tauricum* clades. ITS1 recovered the most clades with statistical support ≥ 70% BS, whereas *trnH-psbA* recovered only the *D. elongatum* clade with strong bootstrap support (84/ 86%).

Genetic distances were generally small in all markers. The ranges of intraspecific versus interspecific pairwise genetic distances overlapped for all markers, except in the combined chloroplast dataset

TABLE 2. Bootstrap values of MP and ML analysis including indels, for clades with more than one sequence. Values for each single markers as well as for the concatenated chloroplast markers (CPall), nrITS1-5.8S-ITS2 (ITS) and the combined sequence data (combined) are shown. Values ≥70% BS are in bold. Dashes denote clades that were absent in the respective phylogenetic reconstruction.

species	*trnT-rps4*	*trnL-trnF*	*psbA-trnH*	*rps19-rpl2*	*rpoB*	ITS 1	ITS 2	CPall	ITSI	combined
Dicranum acutifolium	≤ 50	**85/91**						**73/87**	≤ 50	**88/89**
Dicranum angustum		**83/85**				**72/82**		67/**75**	**81/88**	**96/97**
Dicranum bonjeanii	66/66	≤ 50	≤ 50			**87/94**		52/53	**89/90**	**85/79**
Dicranum brevifolium		≤ 50		≤ 50		**80/72**	**76**/64	55/**71**	**92/92**	**93/96**
Dicranum elongatum	≤ 50		**84/86**			59/61		**92/94**	62/64	**94/98**
Dicranum fragilifolium +										
D. elongatum	52/49				62/**71**	**71**/65	≤ 50	**77/76**	60/62	**92/89**
Dicranum fuscescens	**81/86**									
Dicranum flexicaule	≤ 50	56/53				**75/93**	≤ 50	64/63		**83/81**
Dicranum scottianum	**86/85**	**100/100**	-/ 66		60/62	**84/92**	52/56	**100/100**	**86/90**	**100/100**
Dicranum fuscescens +										
Dicranum flexicaule	≤ 50		-/ 54		61/64		56/60			
Dicranum fuscescens +										
Dicranum flexicaule +										
Dicranum scottianum	**91/95**	**85/86**					**79/77**	**75**/41	**71**/66	**90/89**
Dicranum laevidens		≤ 50		**70**/63	61/**71**	68/-		≤ 50		**78/80**
Dicranum leioneuron	57/**77**	53/**74**	-/53	≤ 50		55/**73**	62/62	**100/100**	**83/90**	**100/100**
Dicranum majus	59/**87**	**89/94**	51/65	≤ 50	≤ 50	**77**/60	72/67	**100/99**	**77/81**	**100/100**
Dicranum scoparium	62/**70**	**91/88**	≤ 50	**82/85**	65/63	60/**70**		**100/100**	≤ 50	**96/99**
Dicranum spadiceum	-/64	**64/87**	56/65	≤ 50	52/58	**100/81**	**100/97**	**99/98**	**99/92**	**99/100**
Dicranum tauricum	**100/99**	**99/99**	≤ 50	**92/100**		**82/78**		**99/100**	69/61	**100/100**

(Table 3). Tables of all nucleotide distances measured are available on request. Furthermore, the comparison of maximum intraspecific versus minimum interspecific genetic distances (Fig. 4) showed greater intraspecific than interspecific distances for a number of pairwise comparisons in every partition (data points below the 1:1 line). Therefore, no clear barcode gap was obtained for all pairwise comparisons, i.e. none of the markers was powerful enough to discriminate all studied species.

Discussion

DNA barcoding in Dicranum and implications for mosses in general— All *Dicranum* species included in this study except *D. fuscescens* were distinguishable based on the combined sequence data of five chloroplast markers and nrITS, with bootstrap support >70% for all clades of species represented by more than one sample (Fig. 1, Table 2). However, an increased sampling of the species represented in this study by one or few specimens would be necessary to confirm their monophyly and infer intra- versus interspecific sequence variation with more confidence. The present results support our earlier study focusing on closely related species within the *D. scoparium* complex (Lang & Stech 2014), namely the close relationship between *D. bonjeanii* and *D. scoparium* and the separation of *D. majus* from the *D. scoparium* complex. In addition, *D. leioneuron*, which was not included in Lang & Stech (2014), is resolved as a member of the *D. scoparium* complex here. As the molecular clades of these species coincide with the morphological species circumscriptions, we conclude that the sequenced entities are in fact separate species. *Dicranum flexicaule* is morphologically very similar to *D. fuscescens* and frequently regarded as a variety or a form of the latter (Ireland 2007; Mönkemeyer 1927; Podpěra 1954; Savicz-Lyubitskaya & Smirnova 1970; The Plant List 2013). However, several other authors accept *D. flexicaule* as a separate yet doubtful species (Bellolio-Trucco & Ireland 1990; Hedenäs & Bisang 2004). The present molecular data support a close relationship of *D. flexicaule* with *D. fuscescens*, and in addition *D. scottianum*, but analyses of a larger number of specimens or additional markers are necessary to resolve their relationships with confidence and conclude about the taxonomic status of *D. flexicaule*.

Each individual locus provided insufficient variability to distinguish all sequenced species (Table 2, Fig. 4). The ITS region as well as the chloroplast markers *trnL-F* and *rps4-trnT* showed the highest species discrimination capacity in terms of statistical support, in accordance with previous studies (e.g., La Farge *et al*. 2002; Hernández-Maqueda *et al*. 2008; Hollingsworth *et al*. 2009). However, the *D. elongatum* clade was only supported by *psbA-trnH* and none of the markers delimited *D. laevidens* (Table 2). The *psbA-trnH* spacer possessed a relatively high proportion of parsimony-informative characters in *Dicranum*, as in other moss species (Liu *et al*. 2010; Hassel *et al*. 2013), although the resulting tree was still poorly resolved (cf. Table 2). Neither the combined chloroplast loci nor the generally variable ITS region could discriminate all included *Dicranum* species with confidence. A recent study of the *Racomitrium canescens* (Hedw.) Brid. complex (Stech *et al*. 2013), another representative of subclass Dicranidae, showed that nrITS performed better in terms of species discrimination capacity than chloroplast data. In *Dicranum*, the concatenated chloroplast markers provided clades with generally better support, which may be due to the larger number of chloroplast markers included here than in the study by Stech *et al*. (2013), which employed solely the *rps4-trnT-trnL* region. Few studies have so far compared the performance of ITS1 vs ITS2 alone as barcoding markers for bryophytes. ITS2 was considered as universal barcode marker for plants and animals because of conserved regions in the adjacent genes, suitable for

TABLE 3 Pairwise Kimura 2-parameter (K2P) distances for ITS, the combined chloroplast markers and different partitions. The upper two rows indicate the ranges of intraspecific and interspecific distances for all *Dicranum* species. The last row indicates the overlap between the maximum intraspecific and minimum interspecific distances.

	trnT-rps4	trnL-trnF	pbA-trnH	rps19-rpl2	rpoB	ITS 1	ITS 2	ITS	CPall	Combi
intra- specific	0-0.0091	0-0.0159	0-0.0144	0-0.0065	0-0.0045	0-0.0116	0-0.0121	0-0.0103	0-0.0118	0-0.0089
inter- specific	0-0.0279	0-0.0391	0-0.0467	0-0.0165	0-0.0177	0-0.0638	0-0.0316	0-0.0627	0.0005-0.0296	0.0015-0.0346
overlap	0.0091	0.0159	0.0144	0.0065	0.0044	0.0116	0.0121	0.0103	0.0112	0.0073

primer design. Additionally, ITS2 had sufficient variability for identification of closely related species (Yao *et al*. 2010) and has proven to be conclusive for some bryophyte taxa, among them also Arctic species (Hassel et al. 2013). In contrast, other studies reported higher variation and species discrimination capacity of ITS1 in bryophytes (Liu *et al*. 2010; Stech *et al*. 2013), which was also the case in *Dicranum* (Table 2). As suggested by Stech *et al*. (2013), further analyses would be necessary in order to infer which part of the ITS region performs best as DNA barcode in bryophytes.

The present study is another example that a combination of several markers may be necessary to identify moss species with confidence based on molecular data. While one marker was sufficient to discriminate two closely related *Orthodontium* species (Rowntree *et al*. 2010), most complexes of closely related species needed several markers to be discriminated at species level (e.g., Carter 2012; Draper & Hedenäs 2009; Medina *et al*. 2012). However, finding the optimal combination of barcoding markers capable of delimiting closely related species is still a major concern in bryophytes and no consensus has been reached yet (Hollingsworth *et al*. 2011; Liu *et al*. 2010; Stech & Quandt 2010). The combination of ITS1 and/or ITS2, *rps4-trnT-trnL*, and *psbA-trnH* seems to be suitable for moss genera with generally low sequence divergence such as *Dicranum* (compared, for example, with its southern Hemisphere sister genus *Dicranoloma* (Renauld) Renauld; Stech *et al*. 2006). Additional markers such as *rps19-rpl2* may be required for certain species. The *rpoB* gene, in contrast, does not provide any additional resolution.

Molecular versus morphological identification of Dicranum specimens from Svalbard— According to the molecular data, the 30 sequenced *Dicranum* specimens from Svalbard belong to five species, *D. acutifolium*, *D. elongatum*, *D. laevidens*, *D. majus*, and *D. spadiceum*. All of them are among the ten species accepted for the archipelago in the checklist by Frisvoll and Elvebakk (1996). The sequenced specimens represent most of the morphological variation of *Dicranum* in the respective sampled habitats and areas on Svalbard, and consequently, most, if not all, *Dicranum* species occurring there. Nonetheless, molecular analysis of an extended sampling across Svalbard would be necessary to assess whether the five other species accepted in the checklist are actually occurring on the archipelago or not, and to confirm the absence of the seven rejected species. Such an extended sampling would require extensive additional fieldwork or PCR amplification and sequencing of older herbarium material. The latter, however, seems to be difficult according to preliminary analyses (unpublished results) of collections from Edgeøya, eastern Svalbard, dating from the 1980s (cf. Hesse *et al*. 2012).

Dicranum species occurring in the Arctic are difficult to identify morphologically, especially in the field, but also microscopically. In few species the diagnostic characters seem to be stable, such as the strong costa and strongly incrassate, short and smooth upper lamina cells of *D. elongatum*, which could be recognized relatively easily. Most species present more variability in their diagnostic characters and are thus more often misidentified. For example, in temperate habitats, *Dicranum majus* is characterized by strongly falcate leaves, prosenchymatous and porose upper lamina cells, furrows on the costa and a double row of guide cells in the lower leaf. These typical characters are much less distinct in High Arctic specimens (Hedenäs *et al*. 2006). High Arctic specimens can therefore readily be mistaken for other species such as *D. scoparium* or *D. spadiceum* (Hedenäs & Bisang 2004; pers. obs.). The most difficult group of species to identify is comprised of *D. angustum*, *D. groenlandicum*, *D. laevidens,* and *D. spadiceum*. *Dicranum spadiceum* has long and narrow leaves ending in a tubular apex. Its leaf margins are slightly denticulate near the apex and the lamina cells are thin-walled and slightly porose. The basal cells are elongate, gradually becoming shorter and irregular, and lack pores, while the typical parenchymatous cells are sometimes restricted to the tip of the lamina. While *D. angustum* and *D. laevidens* are considered synonyms of *D. spadiceum* in The Plant List (2013), the former is distinguished by long, narrow, tubular and acuminate leaves as well as thin-walled and non-porose lamina cells. *Dicranum laevidens* is distinguished by an entire leaf margin as well as incrassate and porose, prosenchymatous lamina cells (Hedenäs & Bisang 2004). According to the molecular data, *D. angustum* and *D. laevidens* are clearly separated from *D. spadiceum* (Figs. 1-3), supporting their status as separate species. All respective Svalbard specimens belong to either *D. laevidens* or *D. spadiceum*, which corresponds well with the conclusions of Frisvoll and Elvebakk (1996) based on morphology that true *D. angustum* may be rare on Svalbard and further study is necessary to delimit *D. angustum* from *D. laevidens* or *D. spadiceum*. Again, additional fieldwork or molecular analysis of (old) herbarium specimens possibly representing *D. angustum* would be necessary. Species boundaries of *D. laevidens* and *D. groenlandicum* remained unclear because of their strong morphological similarities (Bellolio-Trucco & Ireland 1990; Hedenäs & Bisang 2004; Nyholm 1987; Steere 1978; Tuomikoski *et al*. 1973). In the absence of sporophytes, the distinction between the two species is essentially based on the different growth form, as *D. groenlandicum* grows in very dense and *D. laevidens* in looser tufts. Both the reference specimen of *D. groenlandicum* and one Svalbard specimen (Dic_1651) formed dense cushions, but the latter belonged to *D. laevidens* according to the molecular data, whereas the reference specimen was clearly separated molecularly (Figs. 1-3). This is a first indication that the habit may not always be reliable for identifying *D. groenlandicum*, and that in case no other gametophytic diagnostic characters can be found, sterile plants of *D. groenlandicum* can best be identified by DNA barcoding. Examination of supplementary material would be necessary to confirm this result.

Correct species identification is important in various fields of biodiversity assessments, ecology and conservation (Cornelissen *et al*. 2007; Dinnage *et al*. 2012; Steele & Pires 2011; Winter *et al*. 2012). Morphological identification of Arctic mosses requires taxonomic expertise and a combination of several stable characters. However, gametophytic characters often show deviating morphologies (Bellolio-Trucco & Ireland 1990; Hedenäs & Bisang 2004; Hesse *et al*. 2012). In *Dicranum* and many other genera, sporophytic characters are useful to distinguish gametophytically similar species, e.g., *D. groenlandicum* vs. *D. laevidens* and *D. fuscescens* vs. *D.*

flexicaule. Yet, sporophytes are rarely present in Arctic material. Therefore, species identification of Arctic plants of *Dicranum*, as well as of other complex moss species and genera, could greatly benefit from DNA barcoding. In *Dicranum*, identification can be best achieved using a combination of nuclear and plastid DNA sequences. Additional taxon sampling would, however, be necessary to better understand the relationships between morphological variability and genetic variation, solve taxonomic issues and build up a reference sequence database for molecular identification of unknown specimens by local BLAST searches in addition to molecular phylogenetic approaches.